sciendo

DOI: 10.2478/aoj-2000-0012

Original Article

Ultrastructural identification of cells involved in the healing of intramembranous bone grafts in both the presence and absence of demineralised intramembranous bone matrix

Siew Han Chay
BDS, MOrth(HK), MOrth RCS(Edin)
Assistant Professor of Orthodontics
Faculty of Dentistry
National University of Singapore

A. Bakr M. Rabie
BDS, MS, CertOrth, PhD
Associate Professor of Orthodontics
Faculty of Dentistry
University of Hong Kong

Anut Itthagarun
DDS, PhD
Assistant Professor in Paediatric Dentistry
Faculty of Dentistry
University of Hong Kong

Alveolar bone defects are conditions that impede the progress of orthodontic treatment. This study compared the mechanics of the healing of autogenous intramembranous (IM) bone grafts and grafts comprising a mixture of IM and demineralised bone matrix of autogenous intramembranous origin (DBM_{IM}), in an attempt to determine the reliability of each material. Thirty-two New Zealand white rabbits had a single defect created in their skull. Sixteen were grafted with IM bone alone (Group I: autogenous IM), and the other 16 had a combined graft of composite IM sandwiched between two layers of DBM_{IM} (Group II: composite IM-DBM_{IM}). A third group (Group III) of eight rabbits each had two defects created in their skull; one defect was left empty (A: passive control) and the other filled with rabbit-skin collagen (B: active control). In Groups I and II, inflammatory cells were found to be present on Days 1 and 2 of tissue retrieval. The appearance of the mesenchymal cells and preosteoblasts, osteoblasts and osteocytes was earlier (Day 3) in Group II than in Group I (Day 5). In both groups, preosteoblasts, osteoblasts and osteocytes were observed with no cartilage at the intermediate stage. In conclusion, autogenous IM bone grafts and IM bone grafts in the presence of DBM_{IM} healed through an osteogenic ossification route.

Aust Orthod J 2000; 16: 88–97

Key words: bone graft, DBM, intramembranous bone, osteoinduction, ultrastructural

Received for publication: May 1999
Accepted: March 2000

Introduction

The availability of a broad well-rounded alveolar ridge is essential for the success of orthodontic tooth movement and dental implants. Alveolar bone defects caused by trauma or pathology, early loss of teeth or periodontal disease, narrow alveolar ridges and cleft palates are all conditions that will impede the progress of orthodontic treatment, as well as the integrity of dental implants. Therefore, bone grafting is imperative to restore form and function to the alveolar ridge. Understanding the mechanism of the healing of the composite autogenous intramembranous (IM) and demineralised bone matrix of intramembranous bone origin (DBM_{IM}) provides a sound experimental precedent that allows this graft material to become a predictable part of future orthodontic management.

Urist made the seminal discovery that implantation of demineralised lyophilised segments of bone matrix induced new bone formation.[1] The osteoinductive potential of bone matrix is now well known, and the cellular and biochemical changes during bone induction have been well documented.[2–6] Demineralisation is a prerequisite for the osteo-inductive potential of the bone matrix to be expressed because the implantation of mineralised matrix results in the formation of multinucleated giant cells, but no bone induction.[7] The finding that demineralised bone possesses greater osteo-inductive activity than does mineralised bone may be explained by the possibility that bone mineral impedes the release of inductive factors. Demineralisation allows the access of surrounding responsive cells to bone inductive factors, thereby augmenting the inductive potential.[8]

Bone differentiation induced by demineralised bone matrix is a biologic cascade, consisting of chemotaxis and attachment of mesenchymal cells

to the matrix; proliferation of cells; and the differentiation of cartilage, bone and marrow. The key steps are chemotaxis, mitosis and differentiation.[2,3] Subcutaneous implantation of demineralised bone matrix initiates chemotaxis of mesenchymal cells to the implant.[9]

Clinical application of demineralised bone has been attempted by a number of investigators who have reported successful repair of a number of craniofacial defects.[10–12] Rabie and Lie (1996) reported that demineralised endochondral (EC) bone matrix (DBM_{EC}) augmented the healing capacity of autogenous EC bone grafts, and showed that composite autogenous EC and DBM_{EC} (EC-DBM_{EC}) produced 47 per cent more bone than autogenous EC bone alone.[13] This work was the first demonstration of the enhanced integration and bone-induction ability of the autogenous EC bone in the presence of DBM_{EC}. An osteo-inductive factor was extracted and partially purified from bovine IM bone matrix and exhibited a molecular weight different from that of a comparable osteo-inductive/chondro-inductive factor isolated from EC bone.[14] This work demonstrated that osteo-inductive factors could be present in osseous tissues that form initially and completely via IM ossification. Therefore, we hypothesised that DBM prepared from IM bone (DBM_{IM}) should augment the healing of IM autogenous bone as DBM_{EC} augmented the healing of EC bone grafts.

Furthermore, IM bone has been shown to heal directly through the osteogenic route, bypassing a cartilage intermediate stage.[4] Therefore, we expected that demineralised bone matrix prepared from IM bone also heals directly through bone.

The aim of this study was to identify the cells involved in the healing of intramembranous (IM) bone grafts in the presence of demineralised intramembranous bone matrix. This way we could improve our understanding of the enhanced bone-induction ability of the composite IM-DBM_{IM}

Materials and methods

Animals

Thirty-two adult New Zealand White rabbits (3.9 ± 0.4 kg) were used as the experimental model. A total of 32 defects were created in the skulls of rabbits with 16 defects being grafted with IM bone alone and the other 16 defects grafted with composite IM-DBM_{IM}. Both grafts were of autogenous origin. In the control group, 16 defects were created in 8 rabbits, 8 of which were left empty (passive control) and the other 8 filled with rabbit skin collagen (active control).

Preparation of rabbit DBM_{IM} particles

Fresh IM bone was excised from the mandibles and the parietal bones of New Zealand White rabbits, care being taken to avoid the sutures and condyles and thus prevent contamination with chondrogenic-inducing factors. Bone marrow, soft tissue and periosteum were removed, and the bones then cleaned in phosphate-buffered saline with protease inhibitors, and defatted in diethyl ether. The cleaned bones were frozen in liquid nitrogen, and ground using a pre-cooled analytical mill.* The resulting powder was sieved to give a particle size of ≤ 0.25 mm. The bone powder was demineralised following a modified protocol of Reddi and Huggins.[2] Fifty mL of 0. 5 M HCl† plus protease inhibitors were added to eachgram of bone powder and the resulting suspensionwas dialysed‡ against 0. 5 M HCl for three hours, and distilled in H_2O overnight to remove calcium hydroxyapatite from the bone matrix. The resulting powder was then dried before use.

Preparation of rabbit skin collagen

The collagen was prepared from the rabbits' skin. The skin was cleaned with phosphate-buffered saline to remove soft tissue, minced and treated with a series of sodium chloride solutions, distilled water and 4 per cent acetic acid. Then it was lyophilised and dried before use.

Surgical procedures

The animals were premedicated one hour before surgery with oxytetracycline hydrochloride (Tetroxyla:§ 200 mg/mL, 30 mg/kg body weight) and buprenorphine hydrochloride (Hypnorm:‖ 0.3 mL/kg body weight), supplemented with Diazepam (Valium¶ 10: 5 mg/mL, 1 mg/kg body weight). In order to maintain the level of

* IKA Labortechnik.

† Merk, Germany.

‡ Visking tubing, size 5: MW 12kda, Medicell Internal Ltd. UK.

§ Bimeda, Dublin, Ireland.

‖ Janssen Pharmaceutical, Beerse, Belgium.

¶ Roche.

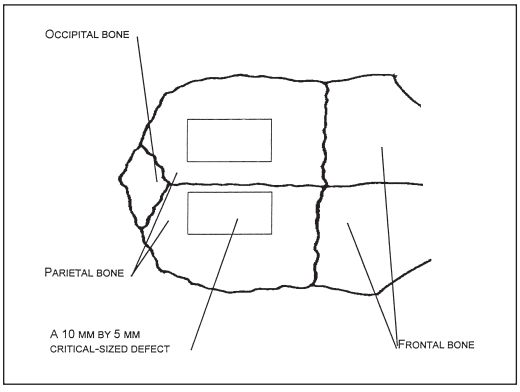

Figure 1. Schematic diagram of dorsal view of skull of rabbit, showing location of two surgically created critical size defects.

neuroleptanalgesia, increments of Hypnorm (01 mL/kg) were given at 30 min intervals during the operation.

The surgical procedures used templates to create 10 x 5 mm^2 full-thickness (approximately 2 mm) cranial defects, devoid of periosteum, in the parietal bones (Figure 1). In the experimental IM bone-graft groups, a piece of cranial IM bone was grafted to the defect. Holes approximately 1 mm in diameter were drilled at opposite ends of the bone grafts and likewise in the parietal bone to allow for fixation of the bone grafts with 0.3 mm diameter stainless steel wires.

Group I: (autogenous IM bone graft). The autogenous IM bone graft was placed into the defect and fixed in place as described above.

Group II: (composite IM-DBM_{IM}. bone graft). The autogenous IM bone graft was sandwiched between two layers of the demineralised intramembranous bone powder, which was mixed with whole blood and fixed in place as described above. (The DBM_{IM} were processed from the mandible of the rabbits.)

Group III: (A: passive control; B: active control). Of the two critical size defects created, one was left empty (A: passive control) and other filled with rabbit-skin collagen (B: active control).

All wounds were closed with 3-0 nylon sutures. No attempts were made to suture the periosteum together.

Post-operative care

Post-operatively, the rabbits were given an antibiotic (Tetroxyla: 30 mg/kg body weight) intramuscularly, daily for ten days, and Temgesic (50 µg/kg daily) for pain relief for fourteen days, as appropriate.

The animals were killed with a lethal dose of sodium pentobarbitone at Days 1, 2, 3, 4, 5, 6, 7 and 14. The defect areas including the surrounding tissue were harvested for histological and ultrastructural preparation.

Tissue preparation for light and electron microscopy

Histological and ultrastructural analyses were performed on tissues obtained at 1, 2, 3, 4, 5, 6, 7 and 14 days after healing.

Tissues were fixed, decalcified in K's Decal Fluid and double embedded in celloidin-paraffin wax. The specimens were cut into serial sections perpendicular to the long axis and 3 µm thick, and stained with haematoxylin and eosin. Histological sections were used to locate the area of the interface between the graft and the host bone on the tissue blocks. The areas of interest were then fixed, postfixed in osmium tetroxide (OsO_4) and trimmed into 1 mm blocks and embedded in resin. Semi-thin sections from the resin block were sectioned and stained with toluidine blue for further orientation and reduction of the block face. Ultrathin sections were cut with a diamond knife to 90 nm and mounted on 200 metal mesh grids. Sections were then stained with Uranyl acetate and Lead citrate and examined with an electron microscope.

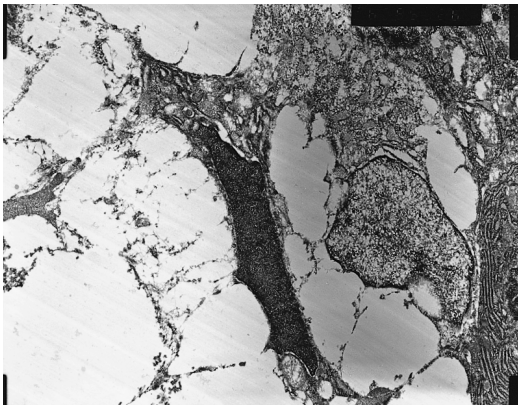

Figure 2. IM bone (Day 4). Electron micrograph of an undifferentiated mesenchymal cell with very thin elongated cytoplasmic process. (x 6,000)

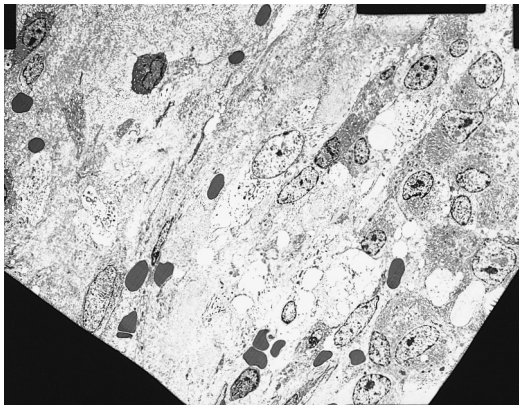

Figure 3a. IM bone (Day 5). Electron micrograph of bone cells including preosteoblasts, osteoblasts and osteocytes involved in the healing of IM bone graft. (x 1,000)

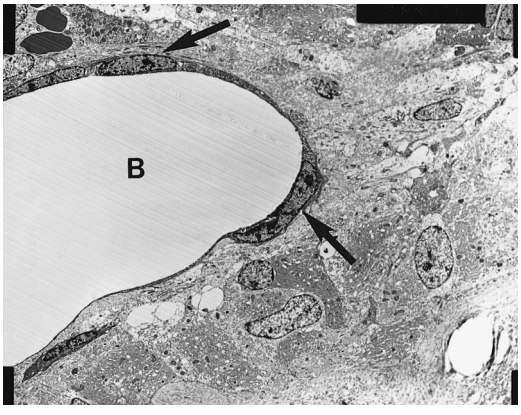

Figure 4. IM bone (Day 5). Electron micrograph of a blood vessel (B) in the newly formed matrix with perivascular mesenchymal cells (arrows). (x 1,500)

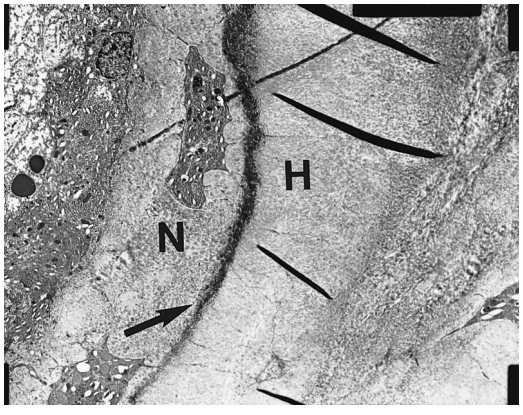

Figure 5. IM bone (Day 6). Electron micrograph of new bone (N) formation next to host bone (H) showing mineralisation front (arrow). (x 2,000)

Results

Clinical and physical examination

All animals remained in excellent health throughout the course of the experiment and rapidly recovered after surgery. There was no evidence of infection or other complications in any animal.

Gross appearance

Both controls (Group III: A and B) did not exhibit bone formation, as they were soft to palpation. In contrast, defects filled with bone grafts were filled with hard tissue.

Histological and ultrastructural findings

The healing in both Groups I and II showed a route of entry for osteoblasts and osteoclasts.

IM-bone-graft group (Group I)

Inflammatory cells (polymorphonuclear leukocytes) were present on Days 1, 2 and 3. Mesenchymal cells were detected on Day 4 (Figure 2) and preosteoblasts, osteoblasts and osteocytes on Day 5 (Figures 3a, b and c). Small blood vessels were seen in the newly formed matrix on Day 5 (Figure 4). New bone formation could be seen next to host bone on Day 6 (Figure 5). More and more osteoblasts were soon surrounded by the bone matrix and became osteocytes (Figure 6).

Localisation of new bone to the host bone-graft interface could be seen in large quantities by Days 7 and 14 (Figure 7). Integration of the IM bone graft with the recipient bed was characterised by the presence of new bone without cartilage.

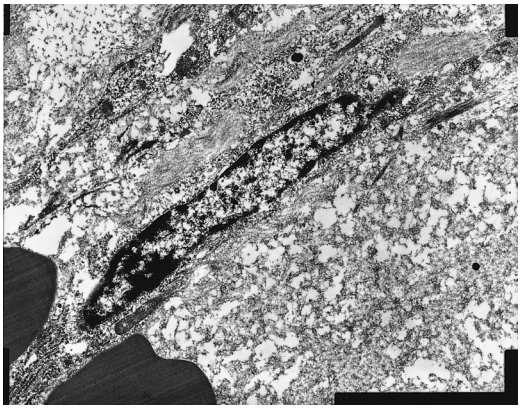

Figure 3b. A preosteoblast with a flattened nuclei and elongated cytoplasm. (x 8,000)

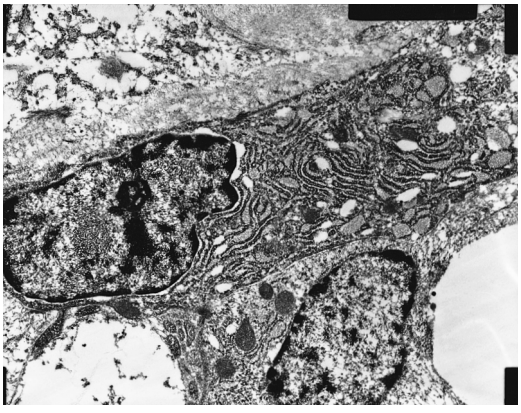

Figure 3c. A full secretory osteoblast with prominent rER and other subcellular organelles. (x 8,000)

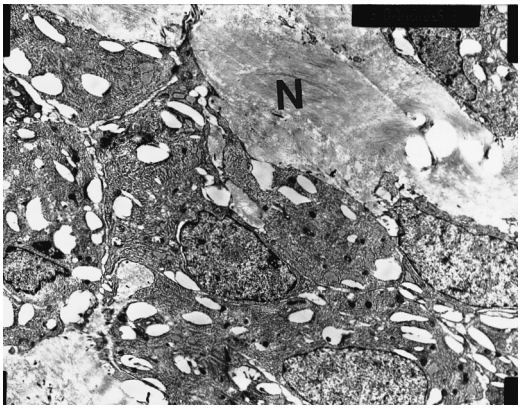

Figure 6. IM bone (Day 7). Electron micrograph of an osteocyte surrounded by bone matrix (N). (x 3,000)

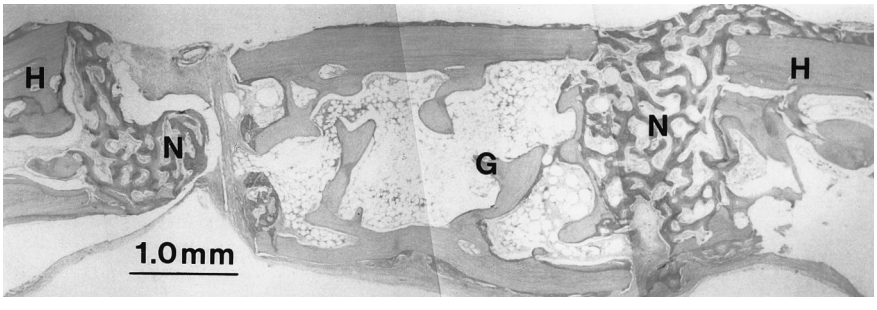

Figure 7. IM bone (Day 14). Photomicrograph of defect grafted with IM bone. Please note new bone (N) bridging from the host bone (H) to bone graft (G). (Stained with PAS) (x 40)

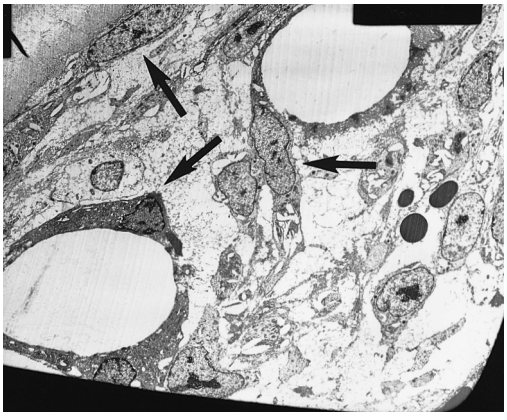

Figure 8. IM-DBM$_{IM}$ bone (Day 3). Electron micrograph of undifferentiated mesenchymal cells (arrows). (x 2,000)

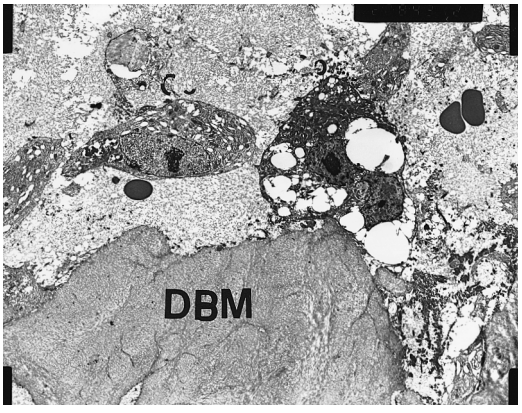

Figure 9a. IM-DBM$_{IM}$ bone (Day 5). Electron micrograph of osteocyte (Oc) and secretory osteoblast cells (Ob) next to DBM. (x 2,000)

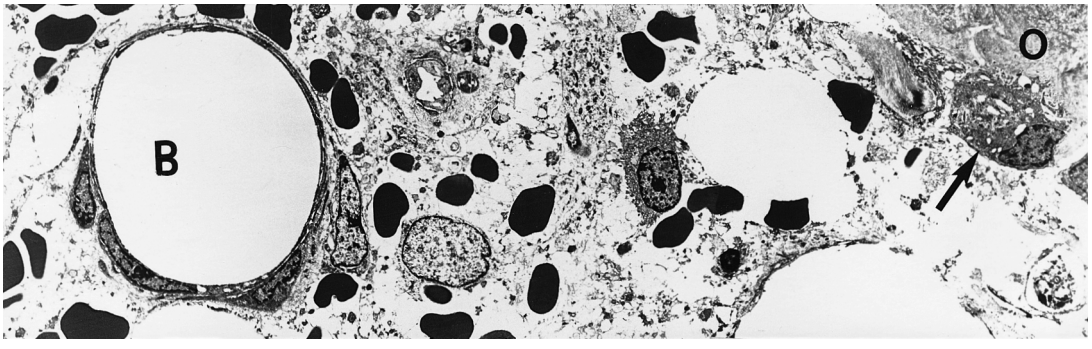

Figure 10. IM-DBM$_{IM}$ bone (Day 7). Composite electron micrograph of healing at interface between host bed and graft. On the left is a blood vessel (B) lined by endothelial cells. A secretory osteoblast (arrow) is seen at the surface of the osteoid (O) (developing bone matrix). (x 2,500)

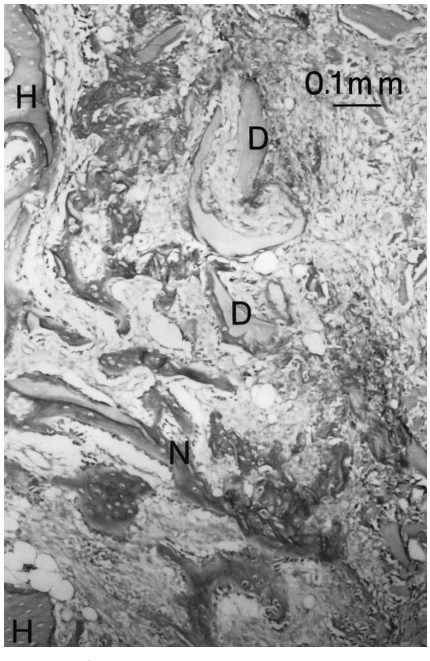

Figure 11b. Higher magnification, showing new bone (N) formed near the host bone (H). DBM$_{IM}$ particles (D) can be seen around. No cartilage was found. (Stained with PAS) (x 100)

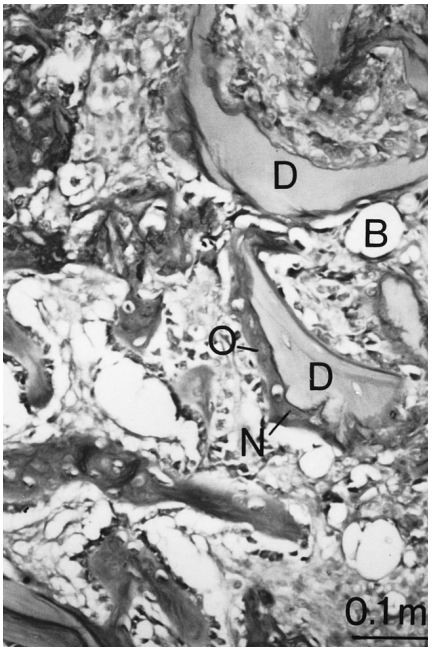

Figure 11c. Higher magnification of Figure 11b, showing new bone (N) induced by DBM$_{IM}$ particles (D) and replacing them. Osteocytes (O) can be found in the new bone. Blood vessels (B) can be seen. No cartilage was found. (Stained with PAS) (x 200)

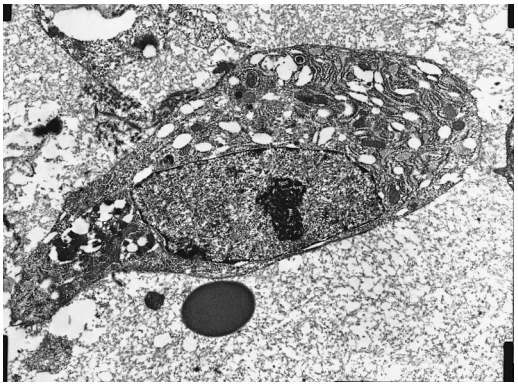

Figure 9b. Higher magnification of the osteocyte cell embedded in bone matrix. (x 5,000)

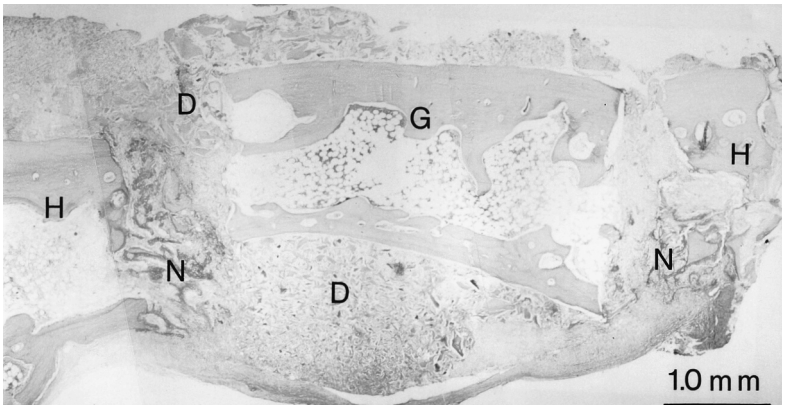

Figure 11a. IM-DBM$_{IM}$ bone (Day 7). Photomicrograph of defect grafted with composite IM-DBM$_{IM}$ bone. New bone (N) was interposed between DBM$_{IM}$ particles (D) between the bone graft (G) and host bone (H). No cartilage was found. (Stained with PAS) (x 40)

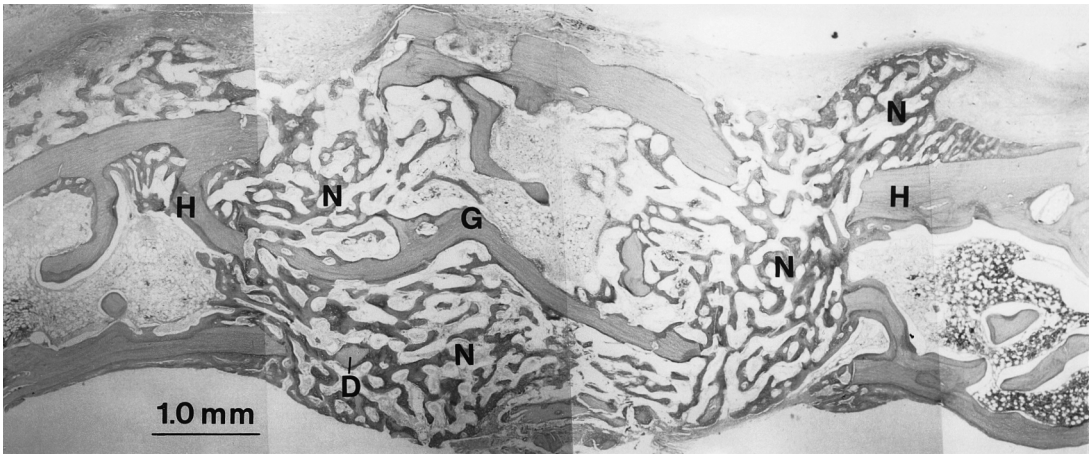

Figure 12. IM-DBM$_{IM}$ bone (Day 14). Photomicrograph of defect grafted with composite IM-DBM$_{IM}$ bone. Abundant new bone (N) interposed between DBM$_{IM}$ particles (D) at all sides of the bone graft (G) and host bone (H). Most of the DBM$_{IM}$ particles were replaced by bone. No cartilage was found. (Stained with PAS) (x 40)

Composite IM-DBM$_{IM}$-bone-graft group (Group III)

Inflammatory cells (polymorphonuclear leukocytes) including macrophages were present on Days 1 and 2, which was similar to the result in the autogenous group. In contrast, the appearances of the mesenchymal cells (Figure 8) and preosteoblasts, osteoblasts and osteocytes was earlier (Days 3 and 4, respectively) than in the healing of autogenous IM bone grafts (Day 5). Appearances of the osteoblasts and osteocytes could be seen next to the DBM (Figure 9a and b). No cartilage cells were detected on Days 7 or 14 (Figures 10, and 11a, b and c).

In the Day-14 specimens (Figure 12), abundant new bone was interposed between DBM$_{IM}$ particles on all sides of the bone graft and host bone. Most of the DBM$_{IM}$ particles were replaced by bone. Amalgamation of the new bone, DBM$_{IM}$ and the bone graft progressed throughout the defect, uniting the graft to the recipient bed. There was a gradient in the amount of new bone formed from the host bed to the graft.

Control groups (Groups IIIA and IIIB)

The defects were filled with fibrous connective tissue (Figure 13). Occasionally, a narrow margin of new bone formation could be seen around the edges of the defects, bridging the marrow space. The collagen graft did not induce bone formation across the defects.

Discussion

In this study, we successfully prepared DBM from IM bone (DBM$_{IM}$) and demonstrated its osteogenic potential.

The rabbit model used in this study was relevant because the non-grafted control defect was found not to heal spontaneously. The area of the defect was large and of the full thickness of the parietal bone. Therefore, in this model, healing must be largely attributed to the implant material.

Reddi and Huggins reported that coarse powders of acid-insoluble matrix of diaphyseal (EC origin) and of calvarial parietal (IM origin) bone rapidly transformed normal fibroblasts into masses of cartilage and bone according to a rigid timetable of sequences.[2] It was concluded that transplants of acid-insoluble residue prepared from the parietal bones yielded typical EC ossification. Scott and Hightower attempted to reproduce these results and demonstrated that EC-bone-derived DBM induced EC ossification, in contrast to IM-bone-derived DBM, which showed no intermediate cartilage.[15] Rabie *et al.,*[4] identified the cells involved in the healing of autogenous IM bone and their data supported those of Scott and Hightower.[15] The difference between Scott and Hightower's results and those of Reddi and Huggins[2] might be due to the manner in which the IM-derived-DBM was prepared. Reddi and Huggins[2] took no special care to avoid perisutural tissues during harvesting of the IM bone; thus, the IM-derived-DBM preparation could have been contaminated with cells capable of chondrogenesis.[16] In the present study, sutures were avoided in the IM bone powder to ensure a pure preparation of IM-derived DBM.

Recently, we reported that composite IM-DBM$_{IM}$ produced more bone than IM bone alone.[6] Therefore, in this study, we compared the healing pattern of IM bone in the presence and absence of DBM$_{IM}$. Integration of bone grafts is dependent on many interrelated processes, including the nature of the host bone and its osteoprogenitor cells, osteoconduction, osteoinduction and the nature of extracellular matrix of the bone graft. As such, in the present work, it was essential to identify the cells involved in the process of bone induction by the IM-DBM$_{IM}$ and to examine the effect of DBM$_{IM}$ on the integration of the bone

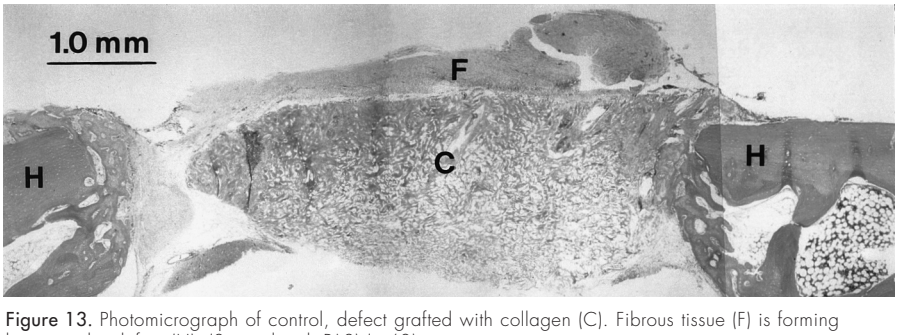

Figure 13. Photomicrograph of control, defect grafted with collagen (C). Fibrous tissue (F) is forming between the defect (H). (Stained with PAS) (x 40)

Table I. Summary of events related to osteogenesis

No. of days post-grafting	Autogenous IM bone graft	Composite IM-DBM_{IM} bone graft
Day 1-2	Inflammatory response Blood clot formation	Inflammatory response Blood clot formation
Day 3	Inflammatory response.	Mesenchymal cell migration and proliferation
Day 4	Mesenchymal cell migration and proliferation	Preosteoblasts, osteoblasts, osteocytes proliferation Appearance of small blood vessels into the newly formed matrix
Day 5	Preosteoblasts,osteoblasts, osteocytes proliferation Appearance of small blood vessels into the newly formed matrix	New bone formation next to the host bone
Day 6	New bone formation next to the host bone	Progress of osteogenesis towards the middle of the defect
Day 7	Progress of osteogenesis towards the middle of the defect	Ongoing dissolution of the implanted matrix. Newly formed bone fills throughout the whole defect
Day 14	Newly formed bone bridges the gap between the host and the bone graft	Newly formed bone bridges the gap between the host and the bone graft

graft with the host bone. Interestingly, the first sign of osteogenesis was seen on Day 4 in the IM bone, whereas it was seen on Day 3 in the composite group. This must be related to the differentiation of undifferentiated mesenchymal cells into osteoblasts. Undifferentiated mesenchymal cells were found to differentiate into osteoblasts when exposed to bone morphogenetic proteins.

The preparation of demineralised bone matrices requires disruption of the gross morphology, architecture and histologic organisation of the donor bones. However, in the present study, it was shown that both the autogenous IM bone and DBM prepared from IM bone origin underwent the same healing process; that is, it has osteogenic potential and produces bone directly bypassing a cartilage intermediate stage (Figures 5, 10, and 11a, b and c). This indicates that the healing must be largely attributable to the biochemical nature of the matrix and not only to the gross morphology and architecture of bone grafts. To date, all commercially available DBM is of endochondral origin and initiates bone induction via EC ossification. DBM_{IM} prepared in this study clearly augmented the bone induction capacity of the IM-autogenous grafts, as well as the recipient bed. Recently, we reported the quantitative data where the composite IM-DBM_{IM} bone grafts produced 204 per cent more new bone than the IM bone alone, when grafted into skull defects.[6]

As expected, healing of the autogenous IM bone graft adopted an IM-ossification route, with the appearance of bone forming cells (preosteoblasts, osteoblasts and osteocytes) bypassing an intermediate cartilage stage (Figures 3a, b and c). The composite IM-DBM_{IM} bone graft presented a mirror image of the healing of autogenous IM bone, except that the appearance of the bone-forming cells and blood vessels was noted earlier (Table I and Figures 8, 9a and b, and 10).

The increased osteoinduction ability of composite IM-DBM_{IM} and the fact that it heals directly through bone, renders it very effective in the repair of defects such as alveolar clefts, ridge augmentation and reconstruction for endosseous implants.

Our results demonstrated that better integration could be achieved between an onlay IM bone graft and the host bone in the presence of DBM_{IM}

(Figures 10, 11a, b and c, and 12). The data presented do not deal directly with measuring the rate of incorporation of a graft; nevertheless, the amalgamation of the new bone with DBM_{IM} particles and the bone graft is indicative of an active state of remodelling and incorporation. Figures 10, 11a, b and c, and 12 of the composite IM-DBM_{IM} show that new bone formation and neovascularisation exist throughout the whole defect, unlike the IM bone graft alone where new bone was localised to the host-bone interface (Figure 7).

Conclusion

Composite IM-DBM_{IM} heals directly through bone. Therefore, DBM_{IM} may have the potential to allow earlier loading of implants and reduce resorption of newly formed bone. Further research in this area needs to be undertaken.

Acknowledgments

This work was supported by C.R.C.Grant 10201960.22311.08003.301.01 and C.R.C.Grant 10201953.15633.08003.301.01.

We thank Dr R. Wong, Dr A.Wong and Miss A. Twitty for their help and guidance; Mr Y. Y. Chui and the late senior technician, Mr M. T. Lee, of the Oral Biology Unit for their excellent technical assistance in the histologic preparation: the staff, especially Annie, of the Laboratory Animal Unit of the University of Hong Kong for their assistance in the care of the animals, and last but not least Dr S. Gang, Dr S. Abbas, Dr D. Leung, Dr Q.L.You, Dr S. Kim and Dr B. Ahmed for their support and assistance in the research.

(This work was a requirement for partial fulfilment of the Masters Degree in Orthodontics at the University of Hong Kong.)

Address for correspondence and reprints:

Dr A. B. M. Rabie
Orthodontics, Faculty of Dentistry,
Prince Philip Dental Hospital
34 Hospital Road
Hong Kong S.A.R.
Email: rabie@hkusua.hku.hu

References

1. Urist MR, Bone: formation by autoinduction. Science 1965; 150: 893–9.
2. Reddi AH, Huggins C. Biochemical sequences in the transformation of normal fibroblasts in adolescent rats. Proc Natl Acad Sci USA 1972; 1601–5.
3. Reddi AH. Cell and biochemistry of endochondral bone development. Coll Relat Res 1981; 1: 209–26.
4 Rabie ABM, Shou D, Samman N. Ultrastructural identification of cells involved in the healing of intramembranous and endochondral bones. Int J Oral and Maxillofac Surg 1996; 25: 383–8.
5. Rabie ABM. Vascular endothelial growth pattern during demineralised bone matrix induced osteogenesis. Connect Tissue Res 1997; 36(4), 337–45.
6. Wong RWK, Rabie ABM. A quantitative assessment of the healing of intramembranous and endochondral autogenous bone grafts. Eur J Orthod 1999; 21: 119–26.
7. Cunningham N, Ma S, Reddi AH. Bone grafts and bone substitutes. In: Habal MB, Reddi AH, eds. Biologic principles of bone induction: Application to bone grafts. Pennsylvania: WB Saunders Company, 1992; 93.
8. Cunningham N, Ma S, Reddi AH. Bone grafts and bone substitutes. In: Habal MB, Reddi AH, eds. Biologic principles of bone induction: Application to bone grafts. Pennsylvania: W Saunders Company, 1992; 94.
9. Weiss RE, Reddi AH. Role of fibronection in collagenous matrix induced mesenchymal cell proliferation and differentiation in vivo. Exp Cell Res 1981; 13: 247–54.
10. Glowacki J, Kaban LB, Murray JE, Folkman J, Mulliken JB. Application of the biological principle of induced osteogenesis for craniofacial defects. Lancet 1981; 1: 959–62.
11. Glowacki J, Mulliken JB. Deminieralised bone implants. Clin Plast Surg 1985; 12: 233–41.
12. Rabie ABM, Comfort MB. Composite grafts in alveolar ridge augmentation for implants. In: Rabie ABM, Urist MR, eds. Bone formation and repair. Amsterdam: Elsiever, 1997; 47.
13. Rabie ABM, Lie KJ. Integration of endochondral bone grafts in the presence of demineralised bone matrix. Int J Oral and Maxillofac Surg 1996; 25: 311–8.
14. Scott CK, Bain SD, Hightower JA. Intramembranous bone matrix is osteo-inductive. Anat Rec 1994; 238: 23–30.
15. Scott CK, Hightower JA. The matrix of endochondral bone differs from the matrix of intramembranous bone. Calcif Tissue Int 1991; 49: 349–54.
16. Rifas L, Vitto J, Memoli VA, Kuettner KE, Henry RW, Peck WA. Selective emergence of differentiated chondrocytes during serum-free cultures of cells derived from fetal rat calvaria. J Cell Biol 1982; 92: 493–504.